Syntheses and Structures of Lithiated Tetramines: $[Li_3(Me_3SiNCH_2CH_2)_3N(THF)_2]$ and $\{(\mu^3\text{-}Cl)Li_3H_4[(Me_3SiNCH_2CH_2)_3N]_2\}$

Zhibang Duan, Victor G. Young, Jr., and John G. Verkade*

Gilman Hall, Department of Chemistry, Iowa State University, Ames, Iowa 50011

Received November 30, 1994[⊗]

The compounds $[Li_3(Me_3SiNCH_2CH_2)_3N(THF)_2]$, **2**, and $\{(\mu^3\text{-}Cl)Li_3H_4[(Me_3SiNCH_2CH_2)_3N]_2\}$, **3**, were synthesized and characterized by ^1H, ^{13}C, ^{29}Si, and ^7Li NMR spectroscopies, and their structures were determined by single crystal X-ray crystallography. Compound **2** was shown to contain a trigonal monopyramidal lithium center while **3** utilizes a LiCl to link two amido triamine ligands together. Crystal data: **2**, triclinic with $a = 9.2035(8)$ Å, $b = 9.579(2)$ Å, $c = 19.881(2)$ Å, $\alpha = 94.98(1)°$, $\beta = 93.27(1)°$, $\gamma = 103.51(1)°$, $V = 1692.4(4)$ Å^3, $Z = 2$, space group $P\bar{1}$, $R = 0.0592$; **3**, trigonal with $a = 12.449(1)$ Å, $b = 12.449(1)$ Å, $c = 28.251(6)$ Å, $V = 3791.7(9)$ Å^3, $Z = 3$, space group $P3_2$, 50:50 $\bar{y}$, $\bar{x}$, z twin, $R = 0.0249$. Variable-temperature ^1H and ^7Li NMR spectral studies reveal a dynamic behavior of **2** in solution. $^1H^1H$ DQF COSY, $^1H^{13}C$-heterocorrelated 2D, and VT NMR experiments confirm that the structure of **3** in solution is the same as that in the solid state.

Introduction

Lithium amide compounds are important in preparative organic and inorganic chemistry as mild deprotonation or amide transfer reagents.[1] Structural studies of such compounds have revealed a variety of interesting atom arrangements (such as stacking or laddering) for these species in solution[2] and in the solid state.[3] The structures of these compounds appear to depend on both the electronic induction properties and the steric requirements of the organic moieties attached to the nitrogen atoms.[4] Thus, for example, the structures of multifunctional amides studied so far have shown rather different patterns of aggregation (such as adamantoid configurations) from those of monofunctional amides.[5,6] Because of this, structural studies on multifunctional lithium amide compounds may provide insights into the origins of their reactivities and reveal additional examples of interesting modes of atom arrangements.

Recently, trifunctional lithium amides of the type $Li_3(RNCH_2CH_2)_3N$ have been utilized as starting materials for synthesizing azametallatranes.[7,8] Among such amides $Li_3(Me_3SiNCH_2CH_2)_3N$, **1**, is one of the most widely used ligands. Because of its bulky nature it can stabilize highly reactive organometallic moieties such as phosphinidenes[9] and terminal selenides and tellurides.[10] To our knowledge, however, no structural investigations have thus far been reported for lithium salts of this or analogous tetramines. As part of our interest in the chemistry of atranes,[11] we have recently described the structural properties of complexes of neutral tripodal ligands such as $(H_2NCH_2CH_2)_3N$, $(MeNHCH_2CH_2)_3N$ and $(HOCH_2CH_2)_3N$, with alkali and alkaline earth cations.[11,12] In broadening these studies, we report here syntheses of the lithiated tetramines $[Li_3(Me_3SiNCH_2CH_2)_3N(THF)_2]$, **2**, and $\{(\mu^3\text{-}Cl)Li_3H_4(Me_3SiNCH_2CH_2)_3N]_2\}$, **3**. Both compounds display novel structural features as shown by X-ray crystallography.

Experimental Section

General Procedures. All reactions were carried out under argon using standard Schlenk or drybox techniques.[13] Solvents were dried over and distilled from Na/benzophenone under nitrogen and stored over 4 Å molecular sieves under an argon atmosphere prior to use. *n*-Butyllithium (2.0 M in cyclohexane) was purchased from Aldrich. $MoCl_4(CH_3CN)_2$,[14] H_3TMS-tren, $[(Me_3SiNHCH_2CH_2)_3N]$,[15] and **1**[7c] were prepared using published methods.

NMR spectra were recorded at 20 °C, unless otherwise stated, on a Nicolet NT 300 (^1H) or a Varian VXR 300 machine with deuterated solvents as an internal lock. ^1H NMR (299.949 MHz) spectra were referenced to the deuterated solvent or Me_4Si as the internal reference. ^{13}C NMR (75.429 MHz) spectra were referenced to solvent signals. A $^1H^1H$ double quantum filtered (DQF) COSY NMR spectrum was acquired on a Unity 500 spectrometer in C_6D_6. $^{29}Si\{^1H\}$ (59.585 MHz) NMR spectra were referenced to TMS in C_6D_6 (20% by volume) as an

[⊗] Abstract published in *Advance ACS Abstracts,* March 15, 1995.

(1) (a) Fieser, M. *Fieser's Reagents for Organic Synthesis*; Wiley-Interscience: New York, 1986; Vol. 12. (b) Lappert, M. F.; Power, P. P.; Sanger, A. R.; Srivastava, R. C. *Metal and Metalloid Amides*; Ellis Horwood-Wiley: Chichester, England, 1980.
(2) (a) Galiano-Roth, A. S.; Michaelides, E. M.; Collum, D. B. *J. Am. Chem. Soc.* **1988**, *110*, 2658. (b) Kallman, N.; Collum, D. B. *J. Am. Chem. Soc.* **1987**, *109*, 7466. (c) Jackman, L. M.; Scarmoutzos, L. M. *J. Am. Chem. Soc.* **1987**, *109*, 5348. (d) Reed, D.; Barr, D.; Mulvey, R. E.; Snaith, R. *J. Chem. Soc., Dalton Trans.* **1986**, 557.
(3) (a) Mulvey, R. E. *Chem. Soc. Rev.* **1991**, *20*, 167 and references therein. (b) Gregory, K.; Schleyer, P. v. R.; Snaith, R. *Adv. Inorg. Chem.* **1991**, *37*, 47 and references therein.
(4) (a) Romesberg, F. E.; Collum, D. B. *J. Am. Chem. Soc.* **1992**, *114*, 2112. (b) Gregory, K.; Bremer, M.; Bauer, W.; Schleyer, P. v. R.; Lorenzen, N. P.; Kopf, J.; Weiss, E. *Organometallics* **1990**, *9*, 1485.
(5) (a) Brauer, D. J.; Bürger, H.; Liewald, G. R. *J. Organomet. Chem.* **1986**, *308*, 119. (b) Brauer, D. J.; Bürger, H.; Liewald, G. R.; Wilke, J. *J. Organomet. Chem.* **1985**, *287*, 305.
(6) (a) Gade, L. H.; Becker, C.; Lauher, J. W. *Inorg. Chem.* **1993**, *32*, 2308. (b) Gade, L. H.; Mahr, N. *J. Chem. Soc., Dalton Trans.* **1993**, 489.
(7) (a) Shih, K.-Y.; Schrock, R. R.; Kempe, R. *J. Am. Chem. Soc.* **1994**, *116*, 8804. (b) Cummins, C. C.; Schrock, R. R.; Davis, W. M. *Inorg. Chem.* **1994**, *33*, 1448. (c) Cummins, C. C.; Schrock, R. R.; Davis, W. M. *Organometallics* **1992**, *11*, 1452. (d) Cummins, C. C.; Lee, J.; Schrock, R. R. *Angew. Chem., Int. Ed. Engl.* **1992**, *104*, 1501.
(8) (a) Duan, Z.; Verkade, J. G. *Inorg. Chem.* **1995**, *34*, 1576. (b) Duan, Z.; Naiini, A. A.; Lee, J.-H.; Verkade, J. G. Submitted.
(9) Cummins, C. C.; Schrock, R. R.; Davis, W. M. *Angew. Chem., Int. Ed. Engl.* **1993**, *32*, 756.
(10) Christou, V.; Arnold, J. *Angew. Chem., Int. Ed. Engl.* **1993**, *32*, 1450.
(11) (a) Verkade, J. G. *Coord. Chem. Rev., Main Group Chem. Rev.* **1994**, *137*, 233. (b) Verkade, J. G. *Acc. Chem. Res.* **1993**, *26*, 483.
(12) Naiini, A. A.; Pinkas, J.; Plass, W.; Young, V. G.; Verkade, J. G. *Inorg. Chem.* **1994**, *33*, 2137.
(13) Shriver, D. F.; Drezdon, M. A. *The Manipulation of Air-Sensitive Compounds*; Wiley-Interscience: New York, 1986.
(14) Dilworth, J. R.; Richards, R. L. *Inorg. Synth.* **1980**, *20*, 119.
(15) (a) Pinkas, J.; Wang, T.; Jacobson, R. A.; Verkade, J. G. *Inorg. Chem.* **1994**, *33*, 4202. (b) Gudat, D.; Verkade, J. G. *Organometallics* **1989**, *8*, 2772. (c) Kupce, E.; Liepins, E.; Zelcans, G.; Lukevics, E. *J. Organomet. Chem.* **1987**, *333*, 1.

0020-1669/95/1334-2179$09.00/0

external standard. ^{7}Li (116.568 MHz) NMR spectra were referenced[16] to LiOD (4 M solution in D_2O) as an external standard. Variable-temperature NMR spectra were measured in toluene-d_8 or benzene-d_6 on a Varian VXR 300 spectrometer with a precision of ±1 °C. Coalescence temperatures were determined by recording a series of spectra taken at incremental temperatures of 2 °C (1 °C increments near the coalescence temperature). Elemental analysis were performed by Desert Analytics, Tucson, AZ. Melting points were measured with a Thomas-Hoover capillary apparatus.

$Li_3(Me_3SiNCH_2CH_2)_3N(THF)_2$, 2. Method A. Compound **1** (0.429 g, 1.13 mmol) was dissolved in 20 mL of THF at 0 °C. After the mixture was stirred at room temperature for 23 h, the solvent was evaporated to dryness *in vacuo*. The residue was extracted with 3 × 8 mL of pentane, and the extractant was concentrated and stored at −30 °C. The colorless product **2** was obtained as crystals which were isolated by filtration and washing with cold pentane and subsequently dried *in vacuo* (81% yield). Anal. Calcd for $C_{23}H_{55}Li_3N_4O_2Si_3$: C, 52.64; H, 10.56; N, 10.68. Found: C, 52.17; H, 10.40; N, 10.45. Mp dec > 137 °C. ^{1}H NMR (C_6D_6): δ 3.51 [m, 8 H, $(CH_2CH_2)_2O$,], 3.25 (t, 6 H, $^3J_{HH}$ = 5.4 Hz, $SiNCH_2$), 2.54 (t, 6 H, $^3J_{HH}$ = 5.4 Hz, $N(CH_2)_3$), 1.25 [m, 8 H, $(CH_2CH_2)_2O$], 0.34 (s, 27 H, CH_3). ^{13}C{^{1}H} NMR (C_6D_6): δ 68.67 [$(CH_2CH_2)_2O$], 56.28 [$N(CH_2)_3$], 44.86 ($SiNCH_2$), 25.33 [$(CH_2CH_2)_2O$], 2.37 (CH_3). ^{7}Li NMR (C_6D_6): −0.38. ^{29}Si NMR (C_6D_6): δ −7.71.

Method B. A solution of Li_3TMS-tren (1.51 g, 3.96 mmol) in 20 mL of THF was added to a stirred suspension of $LaCl_3$ (0.985 g, 4.024 mmol) in 30 mL of THF. The mixture was refluxed for 70 h. After the solvent was removed *in vacuo* to dryness, the residue was extracted by 3 × 8 mL of pentane. The extract was concentrated and stored at −30 °C. Product **2** was obtained as crystals which were isolated by filtration and washing with cold pentane and subsequently dried *in vacuo* (47% yield).

{(μ^3-Cl)Li_3H_4[$(Me_3SiNCH_2CH_2)_3N$]$_2$}, 3. Method A. A solution of *n*-BuLi (2.0 mL, 2.0 M, 4.0 mmol) in cyclohexane was added to a solution of H_3TMS-tren (1.5 g, 4.0 mmol) and LiCl (0.090 g, 2.1 mmol) in 15 mL of THF which was cooled by an ice bath. After the solution was stirred at room temperature for 22 h, the solvent was removed *in vacuo* and 30 mL of pentane was added to the residue. The mixture was stirred at room temperature for another 6 h, filtered, and washed with 3 × 5 mL of pentane. The filtrate and the washings were combined and concentrated to about 8 mL. The solution was stored in a freezer at about −30 °C, and compound **3** was obtained as light yellow crystals which were isolated by filtration and washing with cold pentane and were subsequently dried *in vacuo* (74% yield). Anal. Calcd for $C_{30}H_{82}ClLi_3N_8Si_6$: C, 46.21; H, 10.60; N, 14.37. Found: C, 46.50; H, 10.93; N, 14.23. Mp 119−121 °C. ^{1}H NMR (500 MHz, C_6D_6): δ 3.42 (d, 2 H, J = 12.5 Hz, H_g. For proton subscript labels, see Discussion), 3.28 (t, 2 H, J = 11.0 Hz, $H_{g'}$), 3.04−2.98 (m, 2 H, H_b), 2.95−2.93 (m, 2 H, H_h), 2.85−2.78 (m, 2 H, $H_{b'}$), 2.44−2.27 (m, 10 H, H_e, H_c, H_f, $H_{f'}$, $H_{c'}$), 2.22 (d, 2 H, J = 11.5 Hz, $H_{h'}$), 1.80 (d, 2 H, J = 11.0 Hz, $H_{e'}$), 1.04 (t, 2 H, J = 8.0 Hz, H_a), 0.57 (t, 2 H, J = 7.0 Hz, H_d), 0.32 (s, 18 H, CH_3), 0.17 (s, 18 H, CH_3), 0.15 (s, 18 H, CH_3). ^{13}C{^{1}H} NMR (C_6D_6): δ 60.29 (C_h), 60.01 (C_c), 52.27 (C_f), 44.42 (C_g), 39.62 (C_e), 38.70 (C_b), 2.10 (CH_3), 0.42 (CH_3), −0.57 (CH_3). ^{29}Si-{^{1}H} NMR (C_6D_6): δ 11.40, 2.87, −7.49. ^{7}Li NMR (C_6D_6): δ 0.12, −0.24.

Method B. Pentane (40 mL) was added to a Schlenk flask containing 0.66 g (2.1 mmol) of $MoCl_4(CH_3CN)_2$ and 0.76 g (2.0 mmol) of **1** at about −50 °C. After being warmed to room temperature, the reaction mixture was stirred for 142 h, filtered, and washed with pentane. The filtrate and the washings were combined and concentrated to about 4 mL. The solution was stored in a freezer at about −30 °C, and compound **3** was obtained as light brown crystals which were isolated by filtration and washing with cold pentane and were subsequently dried *in vacuo* (two crops, 68% yield). Despite the coloration, the ^{1}H, ^{13}C, and ^{29}Si NMR spectra revealed only resonances consistent with **3**.

Crystal Structure Analyses of 2 and 3. Crystals of **2** and **3** were mounted on glass fibers on a Siemens P4RA instrument for data collections at 213 K. The cell constants were determined from reflections found from a 360° rotation photograph. Twenty-five reflections in the range of 35−50° in 2θ were used to determine high-angle cell constants. Lorentz and polarization corrections were applied to the data as were nonlinear corrections based on the decay in the standard reflections. A series of azimuthal reflections was collected for both samples and semi-empirical absorption corrections were applied. Crystal data, experimental conditions for data collections, and solution and structure refinement parameters are listed in Table 1.

The space group $P\bar{1}$ was chosen for **2** on the basis of the lack of systematic absences and intensity statistics. This assumption proved to be correct according to a successful direct-methods solution[17] and subsequent refinement. All non-hydrogen atoms were placed directly from the *E*-map. All non-hydrogen atoms were refined with anisotropic displacement parameters. All methylene hydrogens were treated as riding atoms with isotropic displacement parameters fixed 1.2 times the value refined for the respective host atom. Methyl hydrogens were refined as rotating rigid groups with individual group isotropic displacement parameters.

Compound **2** consists of a unit of TMS-tren, three lithium atoms, and two THF molecules. The C(1), C(3), and C(5) carbons are disordered over two sites each in a 0.62:0.38 ratio. Both THF molecules are also disordered, each having two carbon atoms modeled with envelope-flap disorder restraints. These restraints are designed to maintain the nearest neighbor and next nearest neighbor distances for both THF molecules within 0.03 Å esd. Even with these restraints, all the carbon atoms in the THF molecules have high anisotropic displacement parameters. These factors and perhaps poor crystal quality led to a refinement that converged with *R*1 only slightly better than 6.0%.

The solution for **3** was nontrivial. Systematic absences indicated six possible trigonal space groups, $P3_1$, $P3_2$, $P3_121$, $P3_221$, $P3_112$, and $P3_212$. The data merged well for both Laue groups $\bar{3}$ and $\bar{3}m$, but not $\bar{3}1m$, eliminating both $P3_112$ and $P3_212$ as possible choices. An initial model was determined in space group $P3_1$ from a partial direct-methods solution of only the silicon atoms, which was later expanded to include all remaining non-hydrogen atoms using like bond-length restraints to hold the model together. Residuals at this point in the refinement were 28%. No reasonable direct-methods solution could be obtained in space groups $P3_121$ or $P3_221$. However, the $P3_1$ solution was transformed into the space groups by halving the contents and moving the pseudomolecular C_2 axis onto the crystallographic 2 site as required by either $P3_121$ or $P3_221$. This process produced a poorer result than the previous one and was abandoned. It soon became clear that the data collected was from a twinned crystal in either of the enantiomorphic space groups $P3_1$ or $P\bar{3}_2$. The result of twinning causes the data to appear to fit Laue class $\bar{3}m$.[18a] After considerable trial and error, the space group $P3_2$ with a twin element corresponding to a $\bar{y}$, $\bar{x}$, $\bar{z}$ transformation produced the best result. The Flack parameter[19] was used as a gauge to determine which twin combination was correct. Residuals prior to selection of the proper twin were 22%. After the twin was added the residuals dropped to 2.6%. All nonhydrogen atoms were refined with anisotropic displacement parameters. All hydrogens, with the exceptions of H(2N) and H(2N'), were treated as riding atoms with individual or group (methyl) isotropic displacement parameters. The amido hydrogens were allowed to refine positionally while both of their N−H bond lengths were restrained to maintain the same bond length within 0.03 Å. These protons are directed toward the chelated chlorine atom. One methyl group corresponding to C(13) appears to have rotationally disordered hydrogens. It was treated as two half-occupied methyl groups staggered torsionally by 60° with the group isotropic displacement parameter fixed at two times the value for C(13).

Final refinements were done with SHELXL-93.[18b,20] All thermal ellipsoid drawings are presented at 50% probability without hydrogen

(16) (a) Harris, R. K.; Mann, B. E. *NMR and the Periodic Table*; Academic Press: New York, 1978. (b) Jameson, C. J. In *Multinuclear NMR*; Mason, J., Ed.; Plenum Press: New York, 1987.

(17) SHELXTL-PLUS, Siemens Analytical X-ray, Inc., Madison, WI.

(18) *International Tables for Crystallography*; Kluwer Academic Publishers: Dordrecht, The Netherlands, 1992; Vol. C: (a) Tables 1.3.4.1 and 1.3.42; (b) Tables 4.2.6.8 and 6.1.1.4.

(19) (a) Flack, H. D. *Acta Crystallogr.* **1983**, *A39*, 876. (b) Bernardinelli, G.; Flack, H. D. *Acta Crystallogr.* **1985**, *A41*, 500.

(20) SHELXL-93: Sheldrick, G. M. *J. Appl. Crystallogr.*, in preparation.

Table 1. Crystal, Data Collection, Solution, and Structure Refinement Parameters for **2** and **3**

	2	**3**
formula	$C_{23}H_{55}Li_3N_4O_2Si_3$	$C_{30}H_{82}ClLi_3N_8Si_6$
fw	524.80	779.84
cryst size (mm)	0.40 × 0.35 × 0.10	0.35 × 0.30 × 0.25
cryst system	triclinic	trigonal
space group	$P\bar{1}$	$P3_2$ (50% twin component $\bar{y}, \bar{x}, z$)
a (Å)	9.2035(8)	12.449(1)
b (Å)	9.579(2)	12.449(1)
c (Å)	19.881(2)	28.251(6)
α (deg)	94.98(1)	90.0
β (deg)	93.27(1)	90.0
γ (deg)	103.51(1)	120.0
V (Å^3)	1692.4(4)	3791.7(9)
Z	2	3
d_{calcd} (g/cm^3)	1.030	1.025
abs coeff (mm^{-1})	1.457	2.232
F(000)	576	1284
diffractometer	Siemens P4RA	Siemens P4RA
radiation	Cu Kα (λ = 1.541 78 Å)	Cu Kα (λ = 1.541 78 Å)
temp (K)	213(1)	213(1)
monochromator	graphite	graphite
θ range (deg)	4.48−56.87	3.13−56.89
scan type	$\theta-2\theta$	$\theta-2\theta$
index ranges	$-9 \le h \le 9$	$-13 \le h \le 13$
	$0 \le k \le 10$	$-13 \le k \le 13$
	$-21 \le l \le 21$	$0 \le l \le 30$
reflcns collcd	4855	10439
indepdt reflcns	4531	3480
R_{int}	0.0809	0.0574
obsd reflcns	3706 ($I \ge 2\sigma(I)$)	3353 ($I \ge 2\sigma(I)$)
weighting scheme, w^{-1}	$[\sigma^2(F_o^2) + (0.1015P)^2 + 0.9199P]$, where $P = (F_o^2 + 2F_c^2)/3$	$[\sigma^2(F_o^2) + (0.0226P)^2]$, where $P = (F_o^2 + 2F_c^2)/3$
params refined	401	503
final R indices [$I \ge 2\sigma(I)$]	$R1^a = 0.0592$	$R1^a = 0.0249$
	w$R2^b = 0.1632$	w$R2^b = 0.0516$
R indices (all data)	$R1^a = 0.0691$	$R1^a = 0.0264$
	w$R2^b = 0.1709$	w$R2^b = 0.0521$
GOF, obsd and all data	1.137, 1.067	0.991, 0.980
largest and mean Δ/σ	0.004, 0.000	0.004, 0.000
largest diff peak (e/Å^{-3})	0.485	0.138
largest diff hole (e/Å^{-3})	−0.424	−0.143

$^a R1 = \sum||F_o| - |F_c||/\sum|F_o|$. ^{b} w$R2 = [\sum[w(F_o^2 - F_c^2)^2]/\sum[w(F_o^2)^2]]^{1/2}$.

Table 2. Selected Bond Distances (Å) and Angles (deg) for **2**

	Distances		
Li(1)−N(2)	2.008(5)	Li(3)−O(50)	1.939(5)
Li(1)−N(1)	2.029(5)	Li(3)−N(2)	1.965(6)
Li(1)−N(3)	2.036(5)	Li(3)−N(4)	2.095(5)
Li(1)−N(4)	2.193(5)	N(2)−Si(1)	1.679(2)
Li(2)−O(40)	1.936(5)	N(3)−Si(2)	1.683(3)
Li(2)−N(3)	1.962(6)	N(4)−Si(3)	1.692(3)
Li(2)−N(4)	2.084(5)		
	Angles		
N(2)−Li(1)−N(1)	89.1(2)	Si(1)−N(2)−Li(1)	120.3(2)
N(2)−Li(1)−N(3)	150.0(3)	Li(3)−N(2)−Li(1)	74.7(2)
N(1)−Li(1)−N(3)	89.5(2)	Si(2)−N(3)−Li(2)	123.8(2)
N(2)−Li(1)−N(4)	105.4(2)	Si(2)−N(3)−Li(1)	121.3(2)
N(1)−Li(1)−N(4)	84.3(2)	Li(2)−N(3)−Li(1)	75.0(2)
N(3)−Li(1)−N(4)	104.2(2)	Si(3)−N(4)−Li(2)	101.9(2)
O(40)−Li(2)−N(3)	119.8(3)	Si(3)−N(4)−Li(3)	103.5(2)
O(40)−Li(2)−N(4)	125.3(3)	Li(2)−N(4)−Li(3)	137.5(2)
N(3)−Li(2)−N(4)	111.2(2)	Si(3)−N(4)−Li(1)	133.3(2)
O(50)−Li(3)−N(2)	120.9(3)	Li(2)−N(4)−Li(1)	69.3(2)
O(50)−Li(3)−N(4)	124.4(3)	Li(3)−N(4)−Li(1)	68.4(2)
N(2)−Li(3)−N(4)	110.9(3)	N(4)−Si(3)−Li(2)	43.88(13)
Si(1)−N(2)−Li(3)	125.8(2)		

atoms for clarity. Refinement calculations were performed on a Digital Equipment MicroVAX 3100 computer using the SHELXTL-Plus[17] and a DecStation 5000 computer using SHELXL-93.[20] Selected bond distances and bond angles are given in Tables 2 and 3 for **2** and **3**, respectively. The atomic coordinates and equivalent isotropic displacement parameters are collected in Tables 4 and 5 for **2** and **3**, respectively.

Table 3. Selected Bond Distances (Å) and Angles (deg) for **3**

	Distances		
Li(1)−N(4)	2.020(9)	Li(2)−N(4′)	2.000(9)
Li(1)−N(1)	2.076(8)	Li(2)−Cl(1)	2.456(6)
Li(1)−N(3)	2.114(8)	N(2)−Si(1)	1.722(5)
Li(1)−Cl(1)	2.362(7)	N(3)−Si(2)	1.747(4)
Li(1′)−N(4′)	2.014(8)	N(4)−Si(3)	1.699(4)
Li(1′)−N(1′)	2.097(9)	N(2′)−Si(1′)	1.710(5)
Li(1′)−N(3′)	2.099(8)	N(3′)−Si(2′)	1.761(4)
Li(1′)−Cl(1)	2.349(8)	N(4′)−Si(3′)	1.700(4)
Li(2)−N(4)	1.992(9)		
	Angles		
N(4)−Li(1)−N(1)	92.5(3)	N(4′)−Li(2)−Cl(1)	101.7(3)
N(4)−Li(1)−N(3)	114.6(4)	Li(1′)−Cl(1)−Li(1)	136.4(2)
N(1)−Li(1)−N(3)	89.2(3)	Li(1′)−Cl(1)−Li(2)	68.5(3)
N(4)−Li(1)−Cl(1)	105.0(3)	Li(1)−Cl(1)−Li(2)	67.9(3)
N(1)−Li(1)−Cl(1)	125.5(4)	Si(2)−N(3)−Li(1)	120.0(3)
N(3)−Li(1)−Cl(1)	125.8(4)	Si(3)−N(4)−Li(2)	104.2(3)
N(4′)−Li(1′)−N(1′)	92.0(3)	Si(3)−N(4)−Li(1)	123.6(3)
N(4′)−Li(1′)−N(3′)	114.5(4)	Li(2)−N(4)−Li(1)	84.3(3)
N(1′)−Li(1′)−N(3′)	88.3(3)	Si(2′)−N(3′)−Li(1′)	119.1(3)
N(4′)−Li(1′)−Cl(1)	105.0(3)	Si(3′)−N(4′)−Li(2)	103.4(3)
N(1′)−Li(1′)−Cl(1)	122.7(4)	Si(3′)−N(4′)−Li(1′)	123.5(3)
N(3′)−Li(1′)−Cl(1)	128.6(4)	Li(2)−N(4′)−Li(1′)	84.8(3)
N(4)−Li(2)−N(4′)	155.7(4)	N(4′)−Si(3′)−Li(2)	42.0(2)
N(4)−Li(2)−Cl(1)	102.6(3)		

Results and Discussion

Syntheses. Compound **2** was first obtained accidentally from a reaction which was expected to give a lanthanum azatrane (see Experimental Section). A rational synthesis of **2** was

Table 4. Atomic coordinates ($\times 10^4$) and Equivalent Isotropic Displacement Parameters (Å^2 $\times$ 10^3) for **2**

atom	*x*	*y*	*z*	*U*(eq)[a]
Li(1)	−666(5)	4371(5)	2276(2)	35(1)
Li(2)	−1064(6)	5647(5)	3337(3)	45(1)
Li(3)	1405(6)	5910(6)	1804(3)	50(1)
N(1)	−2075(3)	5375(3)	1797(1)	43(1)
C(1A)	−2225(12)	4526(11)	1132(5)	49(2)
C(1B)	−1920(28)	5158(27)	1087(9)	79(7)
C(2)	−812(5)	4360(5)	879(2)	73(1)
N(2)	209(3)	4023(3)	1392(1)	42(1)
Si(1)	855(1)	2540(1)	1224(1)	45(1)
C(11)	1936(6)	2269(6)	2009(3)	99(2)
C(12)	2105(6)	2596(5)	516(3)	101(2)
C(13)	−660(5)	863(4)	988(3)	87(1)
C(3A)	−3377(12)	5105(11)	2177(5)	50(2)
C(3B)	−3581(20)	4635(28)	1972(10)	86(8)
C(4)	−3596(4)	3822(4)	2543(2)	65(1)
N(3)	−2236(3)	3741(3)	2941(1)	38(1)
Si(2)	−2346(1)	2215(1)	3316(1)	49(1)
C(21)	−482(6)	2342(7)	3783(4)	124(2)
C(22)	−2850(8)	544(5)	2729(3)	109(2)
C(23)	−3711(6)	1915(5)	3980(2)	84(1)
C(5A)	−1280(8)	6910(6)	1777(3)	41(2)
C(5B)	−1840(20)	6861(11)	2119(12)	89(7)
C(6)	−395(4)	7500(3)	2438(2)	55(1)
N(4)	516(3)	6565(2)	2692(1)	37(1)
Si(3)	2052(1)	7233(1)	3237(1)	48(1)
C(31)	1869(6)	6412(7)	4056(2)	116(2)
C(32)	3739(5)	6739(6)	2910(3)	92(2)
C(33)	2529(6)	9237(5)	3442(3)	106(2)
O(40)	−1845(3)	6701(2)	4049(1)	62(1)
C(41A)	−1752(37)	8171(16)	4209(15)	112(15)
C(41B)	−1586(22)	8183(12)	4307(11)	119(8)
C(42A)	−2399(34)	8321(14)	4866(11)	89(8)
C(42B)	−2981(25)	8283(14)	4637(11)	126(6)
C(43)	−3382(7)	6937(8)	4922(3)	121(2)
C(44)	−2922(6)	5913(5)	4453(3)	103(2)
O(50)	2688(3)	7213(2)	1271(1)	61(1)
C(51)	3674(5)	6745(4)	828(2)	70(1)
C(52A)	4899(16)	8106(14)	807(14)	97(6)
C(52B)	4309(22)	8011(11)	453(7)	79(4)
C(53)	4163(7)	9246(6)	871(3)	121(2)
C(54A)	3044(28)	8767(16)	1360(15)	181(14)
C(54B)	2815(16)	8697(12)	1209(9)	89(6)

[a] Equivalent isotropic *U* defined as one-third of the trace of the orthogonalized U_{ij} tensor.

carried out according to reaction 1. Interestingly, the solubility

$$\underset{\mathbf{1}}{Li_3(Me_3SiNCH_2CH_2)_3N} + 2THF \xrightarrow[81\%]{THF} \mathbf{2} \qquad (1)$$

of **2** is quite different from its precursor **1**. The latter is almost insoluble in pentane[7c] while the former is highly soluble in hydrocarbon solvents.

Like **2**, compound **3** was also at first obtained accidentally. In reactions of $MoCl_4(CH_3CN)_2$ with **1** (see Experimental Section and ref 8a) aimed at making $ClMo(Me_3SiNCH_2CH_2)_3N$ (which was very recently reported[7a]), **3** was isolated as light brown crystals in 68% yield. While $MoCl_4(CH_3CN)_2$ functions as the chloride source ion in this reaction, the origin of the protons is not clear. Reaction 2 constitutes a rational synthesis

$$2(Me_3SiNHCH_2CH_2)_3N + LiCl + 2n\text{-}BuLi \xrightarrow[74\%]{THF} \mathbf{3} \qquad (2)$$

of **3**. Although **3** is soluble in hydrocarbon solvents, no **3** could be identified when the reaction was carried out in pentane, apparently owing to the insolubility of LiCl in pentane.

Structural Considerations. Compound **2** (Figure 1) features

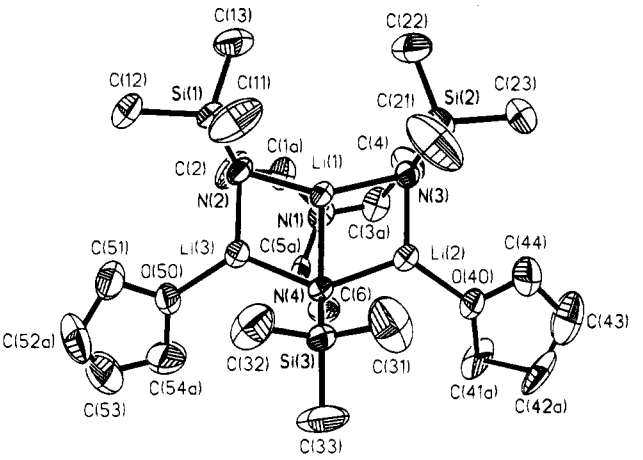

Figure 1. Thermal ellipsoid drawing of **2**. Ellipsoids are drawn at the 50% probability level.

a pseudo C_s symmetry plane that passes through atoms N(1), Li(1), and N(4). Li(1) is four-coordinate while Li(2) and Li(3) are three-coordinate with all three metal atoms lying in the plane defined by N(3), N(4), and N(2). The mean deviation of an atom from this plane is 0.0392 Å. This type of aggregation is similar to the ladder structures found in some lithium amide compounds.[3] Unique, however, is the coordination of Li(1) by N(1) from below the plane in **2**, thus giving Li(1) a trigonal monopyramidal (TMP) coordination geometry as illustrated in the following somewhat idealized structure:

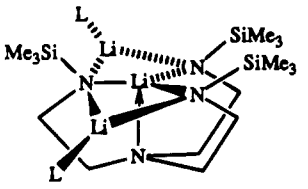

L = THF
2

To our knowledge, this is the first example of this geometry for lithium. In general, this coordination geometry is rare for both main group and transition metal elements, and only five such compounds have been structurally characterized.[7b,7d,15a,21] The coordination geometry of Li(1) deviates from ideal TMP geometry because of the unequal bond angles (N(2)Li(1)N(3) = 150.0(3)°, N(2)Li(1)N(4) = 105.4(2)°, N(3)Li(1)N(4) = 104.2(2)°) in the pseudotrigonal plane which can be attributed to steric interactions between the trimethylsilyl groups on N(2) and N(3) (Figure 1).

Another interesting feature of the structure of **2** is the presence of a five-coordinate nitrogen (N(4)). Five-coordinate environments for nitrogen have been reported for eight lithium amide compounds[5,6b,22] and in several sodium amide complexes.[23] In the previously reported lithium examples to be discussed in more detail shortly, the pentacoordinate nitrogen is bonded to three Li atoms and two carbon and/or silicon substituents. Moreover,

(21) (a) Schumann, H.; Hartmann, U.; Wasserman, W.; Just, O.; Dietrich, A.; Pohl, L.; Hostalek, M.; Lokai, M. *Chem. Ber.* **1991**, *124*, 1113. (b) Schumann, H.; Hartmann, V.; Dietrich, A.; Pickardt, J. *Angew. Chem., Int. Ed. Engl.* **1988**, *27*, 1077. (c) Mealli, C.; Sacconi, L. J. *Chem. Soc., Chem. Commun.* **1973**, 886.

(22) Barr, D.; Clegg, W.; Hodgson, S. M.; Lamming, G. R.; Mulvey, R. E.; Scott, A. J.; Snaith, R.; Wright, D. S. *Angew. Chem., Int. Ed. Engl.* **1989**, *28*, 1241.

(23) (a) Lorenzen, N. P.; Kopf, J.; Olbrich, F.; Schümann, U.; Weiss, E. *Angew Chem., Int. Ed. Engl.* **1990**, *29*, 1441. (b) Brauer, D. J.; Bürger, H.; Geschwandtner, W.; Liewald, G. R.; Krüger, C. *J. Organomet. Chem.* **1983**, *248*, 1.

Table 5. Atomic Coordinates ($\times 10^4$) and Equivalent Isotropic Displacement Parameters (Å^2 $\times$ 10^3) for **3**

atom	*x*	*y*	*z*	*U*(eq)[a]
Li(1)	637(7)	168(7)	−48(3)	37(2)
Li(1′)	−1407(7)	2169(7)	69(3)	40(2)
Li(2)	−1647(7)	−112(7)	15(3)	36(2)
Cl(1)	308(1)	1877(1)	−13(1)	36(1)
N(1)	1195(3)	−513(3)	514(1)	31(1)
C(1)	2031(5)	194(5)	910(2)	47(1)
C(2)	1873(6)	1247(5)	1091(2)	58(2)
N(2)	2494(5)	2360(4)	814(2)	56(1)
Si(1)	3806(1)	3690(1)	995(1)	48(1)
C(11)	4257(11)	4788(7)	502(2)	159(5)
C(12)	5045(7)	3329(8)	1126(3)	106(3)
C(13)	3576(6)	4428(6)	1521(2)	72(2)
C(3)	1740(4)	−1137(4)	240(2)	40(1)
C(4)	2618(5)	−291(5)	−140(2)	44(1)
N(3)	1942(3)	29(3)	−484(1)	36(1)
Si(2)	2737(1)	1143(1)	−921(1)	43(1)
C(21)	3573(6)	648(6)	−1329(2)	78(2)
C(22)	3829(6)	2590(6)	−610(2)	72(2)
C(23)	1565(6)	1346(6)	−1256(2)	62(2)
C(5)	−31(5)	−1399(5)	698(2)	39(1)
C(6)	−1011(4)	−2120(4)	320(2)	38(1)
N(4)	−1079(3)	−1342(3)	−56(1)	31(1)
Si(3)	−1794(1)	−2133(1)	−557(1)	38(1)
C(31)	−924(6)	−2758(6)	−896(2)	62(2)
C(32)	−2023(5)	−1058(5)	−945(2)	58(2)
C(33)	−3352(5)	−3547(6)	−453(2)	68(2)
N(1′)	−2134(3)	2692(4)	−498(1)	40(1)
C(1′)	−1464(5)	3525(5)	−901(2)	51(1)
C(2′)	−392(5)	3411(6)	−1091(2)	61(2)
N(2′)	738(4)	4095(5)	−826(2)	59(1)
Si(1′)	2026(1)	5399(1)	−1026(1)	49(1)
C(11′)	3269(7)	5782(10)	−601(3)	136(4)
C(12′)	1738(8)	6701(7)	−1083(4)	127(4)
C(13′)	2478(7)	5132(7)	−1620(3)	103(3)
C(3′)	−2790(5)	3214(5)	−227(2)	50(1)
C(4′)	−1939(5)	4114(5)	147(2)	50(1)
N(3′)	−1579(4)	3463(3)	491(1)	41(1)
Si(2′)	−401(1)	4356(1)	902(1)	45(1)
C(21′)	−928(7)	5218(6)	1288(2)	82(2)
C(22′)	1005(5)	5404(5)	562(2)	70(2)
C(23′)	−161(7)	3237(6)	1252(2)	71(2)
C(5′)	−3011(5)	1426(5)	−676(2)	45(1)
C(6′)	−3690(4)	468(5)	−288(2)	49(1)
N(4′)	−2893(3)	446(3)	82(1)	37(1)
Si(3′)	−3668(1)	−272(1)	585(1)	50(1)
C(31′)	−4251(7)	614(6)	934(2)	84(2)
C(32′)	−2611(6)	−502(6)	981(2)	68(2)
C(33′)	−5080(6)	−1829(6)	480(3)	91(2)

[a] Equivalent isotropic *U* defined as one-third of the trace of the orthogonalized U_{ij} tensor.

each Li atom is connected to three N atoms. In contrast, the five-coordinate nitrogen atom in **2** is bonded to two three-coordinate Li atoms, one four-coordinate Li atom, and two nonmetallic substituent groups. It is also the first example of nitrogen pentacoordination in which the nitrogen atom coordinates to three lithium atoms located in same plane. Generally, bond lengths increase with coordination numbers (CN), and this is also the case for **2**. The average amido lithium N(CN5)−Li(CN3) bond length of 2.090(5) Å is shorter than the N(CN5)−Li(CN4) bond length (2.193(5) Å) (see Table 2), within experimental error of that reported for $[(t\text{-BuNLi})_2SiMe_2]_2$ (2.075(6) Å[5,9]), and somewhat longer than the N(CN5)−Li(CN3) lengths reported for $\{H_3CC[CH_2N(Li)CH(CH_3)_2]_3\}_2$ (2.031(5) Å[6b]), $\{H_3CC[CH_2N(Li)Si(CH_3)_3]_3\}_2$ (2.039(4) Å[6b]), $[(t\text{-BuNLi})_3SiPh]_2$ (2.039(4) Å[5a]), $[MeSi(NLiSiMe_3)_3]_2$ (2.04(2) Å[5b]), $[Me_3CSi(NLiSiMe_3)_3]_2$ (2.05(1) Å[5b]), $[PhSi(NLiSiMe_3)_3]_2$ (2.057(7) Å[5b]), and $[H_2C(CH_2)_5NLi]_6$ (2.06(2) Å[22]). Similarly, the average amido lithium N(CN4)−Li(CN3) bond distance of 1.964(6) Å is shorter than the average N(CN4)−Li(CN4) bond

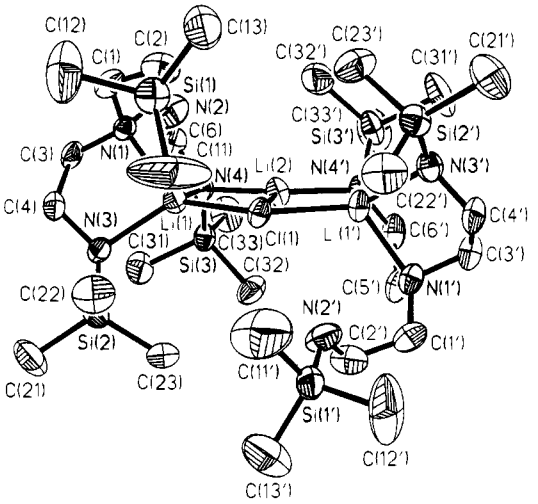

Figure 2. Thermal ellipsoid drawing of **3**. Ellipsoids are drawn at the 50% probability level.

distance (2.022(5) Å) in **2**. It is interesting to note that the transannular bond Li(1)−N(1) (2.029(5) Å) in **2** is shorter than the average amido lithium bond length for both N(CN5)−Li(CN3) and N(CN5)−Li(CN4), comparable with that for N(CN4)−Li(CN4), and somewhat longer than that for N(CN4)−Li(CN3) in this compound. The C−N(CN5)−Si bond angle of 121.5(2)° in **2** is smaller than the average of the angles reported for $[(t\text{-BuNLi})_3SiPh]_2$ (132.9(1)°[5a]) and $[(t\text{-BuNLi})_2SiMe_2]_2$ (125.5(2)°[5a]) and larger than in $\{H_3CC[CH_2N(Li)Si(CH_3)_3]_3\}_2$ (108.1(3)°[6b]).

Compound **3** exhibits pseudo C_2 symmetry with the axis passing through Li(2)−Cl(1) bond, as shown in the somewhat idealized structure in Figure 2. Interestingly, LiCl appears to serve as a binding agent for linking two amido triamine ligands together, as depicted below:

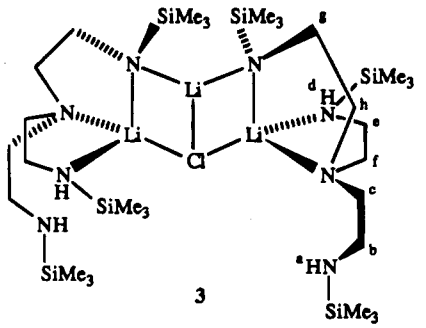

3

Like **2**, **3** also shows two lithium coordination environments, namely, tetrahedral geometries for Li(1) and Li(1′) and a distorted trigonal planar coordination environment for Li(2). Atoms Li(1), Cl(1), Li(1′), N(4′), Li(2), and N(4) are positioned in a plane in which the mean deviation from the plane is 0.0226 Å. It is interesting to note that one of the terminal secondary amine arms of each amido triamine ligand remains uncoordinated while the other coordinates to a lithium. This is confirmed by its solution ^{1}H NMR spectrum which is discussed later. The average tertiary amine−lithium N(CN4)−Li(CN4) bond distance of 2.087(9) Å is comparable with the average secondary amine-lithium [N(CN4)−Li(CN4)] bond distance (2.107(8) Å) in **3**, somewhat longer than the average amido lithium N(CN4)−Li(CN4) distance (2.017(9) Å) which is within experimental error of that for N(CN4)−Li(CN3) (1.996(9) Å) (see Table 3), and slightly longer than the corresponding transannular bond length (2.029(5) Å) in **2**. The average amido−lithium N(CN4)−Li(CN4) bond distance in **3** is comparable to that in **2** while

the average amido lithium N(CN4)−Li(CN3) bond distance in **3** is within experimental error of that in **2**. It is worth noting that the Cl−Li(CN3) bond length of 2.456(6) Å is longer than the average Cl-Li(CN4) bond length of 2.356(8) Å, which is contrary to expectation.

Very recently, the crystal structure of [{MeN(CH_2CH_2-NMe_2)$_2$Li}$_2$Cl][HC{$SiMe_2N(4\text{-}CH_3C_6H_4)$}$_3$Sn], **4**, was communicated.[24] The average tertiary amine−lithium N(CN4)−Li(CN4) bond length (2.11(2) Å) in **4** is somewhat longer than the transannular bond N(CN4)−Li(CN3) (2.029(5) Å) in **2** and comparable with the average tertiary amine−lithium N(CN4)−Li(CN4) bond distance (2.087(9) Å) in **3**. However, the average Cl(CN2)−Li(CN4) bond distance in **4** (2.25(1) Å[24]) is shorter than the Cl(CN3)−Li(CN3) and the average Cl(CN3)−Li(CN4) bond lengths in **3**. These observations probably find their origin in the smaller coordination number of the Cl atom in **4** than in **3**.

NMR Spectra. In solution, the ^1H, $^{13}C\{^1H\}$, $^{29}Si\{^1H\}$, and ^7Li NMR spectra of **2** recorded in C_6D_6 at room temperature reveal patterns corresponding to 3-fold symmetry, which is common for many azametallatranes in the solid and solution states.[7−9] However, this result for **2** is inconsistent with its crystal structure which possesses a pseudomirror plane (Figure 1). On the the basis of the structure of **2** in the solid state, two methyl and four methylene proton resonances would be expected. The variable-temperature ^1H NMR spectra of **2** in toluene-d_8 provide evidence for an exchange process, however. At room temperature, the resonance pattern in this solvent is similar to that observed in C_6D_6 (see Experimental Section). With decreasing temperature, each methylene proton resonance broadens, decoalescing at −50 °C, and splitting into two pairs of broad resonances at 3.26, 3.05 ppm and at 2.72 and 2.51 ppm with integration ratios of 2:1 and 1:2, respectively, at −78 °C. Similar observations were made for the methyl proton resonances. However, we were not able to reach the low-temperature-limiting spectrum because of poor resolution, probably owing to insolubility of **2** at low temperature. The VT ^7Li NMR spectra also reveal the exchange process observed by ^1H NMR spectroscopy. At 20 °C, the ^7Li NMR spectrum of **2** shows only a peak at −0.20 ppm. This peak broadens at −35 °C and decoalesces at −42 °C. Below −44 °C, this peak splits into two peaks, and at −70 °C, two peaks are observed at 1.26 and −0.65 ppm with an approximate integration ratio of 1:2, respectively. The low-temperature ^1H and ^7Li NMR data are consistent with the solid state structure. It is suggested that the fluxionality of **2** observed at higher temperature involves the dissociation of one or both THF molecules followed by (or simultaneous with) the movement of the bridgehead lithium to an exocyclic position as depicted in **6** in Scheme 1. The two-coordinate lithium from which the THF dissociated could then move into the bridgehead position either subsequent to the generation of **6** (or, perhaps more likely, in concert with its formation) to regenerate a molecule of **5**, which could then in turn react with THF to re-form **2**. The free energy of activation for the fluxional process, $\Delta G_c^{\ddagger}$, calculated on the basis of the coalescence temperature from the ^7Li NMR data,[25] is found to be 44.2 ± 0.5 kJ/mol.

The ^1H NMR spectrum of **3** exhibits a complicated pattern in which the 12 diastereotopic methylene proton signals show an array of partially overlapped multiplets. The NH proton signals were located on the basis of $^1H^{13}C$-heterocorrelated 2D and $^1H^1H$ DQF COSY NMR data. Three $SiMe_3$ resonances representing the three inequivalent $SiMe_3$ groups appear in the ^1H, ^{13}C, and ^{29}Si NMR spectra. In contrast to its poorly resolved ^1H NMR spectrum, the $^{13}C\{^1H\}$ NMR spectrum of **3** clearly shows six methylene carbon signals and its ^7Li NMR spectrum displays two resonances (0.12 and −0.24 ppm) with an integration ratio of 1:2, respectively. These data are consistent with the solid state structure of **3**. The absence of evidence for a dynamic process at elevated temperatures (up to 65 °C in C_6D_6) indicates that **3** maintains its solid state molecular configuration remarkably well in solution.

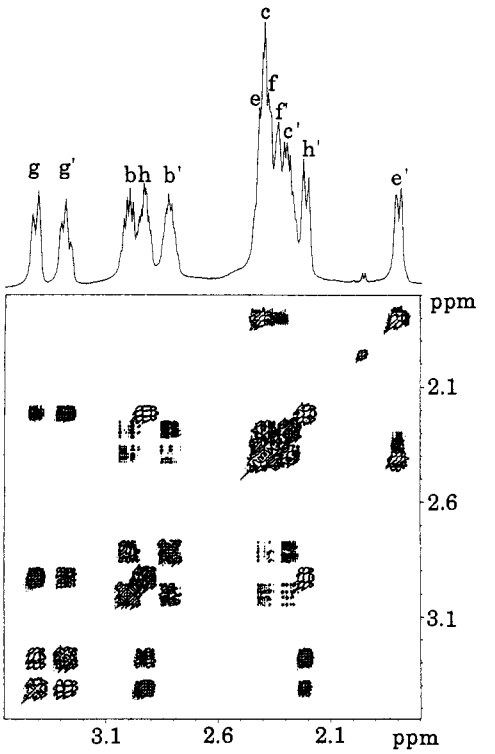

Figure 3. ^1H NMR spectrum of **3** showing 12 methylene proton signals and the ^1H, ^1H DQF COSY 2D NMR spectrum of **3**.

Scheme 1

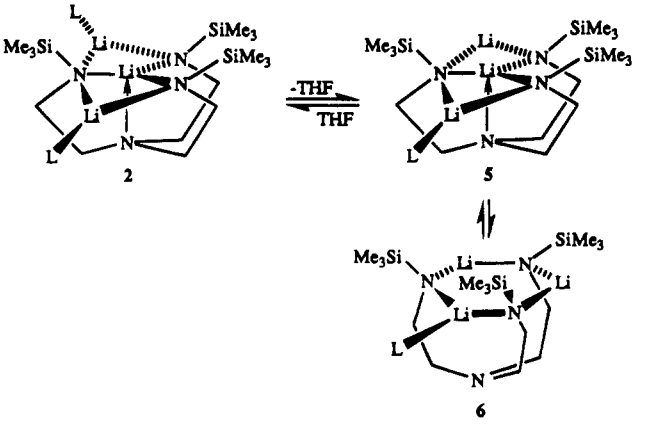

The assignments of the ^1H and $^{13}C\{^1H\}$ NMR signals of **3** are based on $^1H^{13}C$-hetercorrelated 2D and $^1H^1H$ DQF COSY NMR spectra. The ^1H NMR spectrum of **3** in the methylene proton region is shown in Figure 3 together with the result of the $^1H^1H$ DQF COSY experiment. By analysis of the cross-peak pattern and the integrals of individual multiplets, 12 methylene proton signals can be identified. These patterns can be divided into three groups (b, b′, c, c′/e, e′, f, f′/g, g′, h, h′) associated with the three inequivalent arms in each amido triamine ligand expected from the C_2 symmetry of **3**. Using

(24) Hellman, K. W.; Steinert, P.; Gade, L. H. *Inorg. Chem.* **1994**, *33*, 3859.
(25) Sandstrom, J. *Dynamic NMR Spectroscopy*; Academic Press: London, 1982.

Table 6. Correlations between ^1H and ^{13}C NMR Chemical Shifts in **3**

$\delta(^{13}C)$ (ppm)	$\delta(^1H)$ (ppm) (assgnt)[a]	carbon atom[a]
	Methyl Groups	
−0.57	0.17 (CH_3)	CH_3
0.42	0.15 (CH_3)	CH_3
2.10	0.32 (CH_3)	CH_3
	Methylene Groups	
38.70	3.04−2.98 (H_b), 2.85−2.78 ($H_{b'}$)	C_b
39.62	2.42−2.41 (H_e), 1.80 ($H_{e'}$)	C_e
44.42	3.42 (H_g), 3.28 ($H_{g'}$)	C_g
52.27	2.38−2.36 (H_f), 2.35−2.33 ($H_{f'}$)	C_f
60.01	2.41−2.39 (H_c), 2.30−2.27 ($H_{c'}$)	C_c
60.29	2.95−2.93 (H_h), 2.22 ($H_{h'}$)	C_h

[a] For atom-labeling scheme, see structural depiction for **3** in Discussion.

2D NMR data along with a knowledge of the structure of **3**, specific assignments of all of the ^1H and ^{13}C signals can be achieved, except for the $SiMe_3$ groups. Cross-peaks in the $^1H^{13}C$-heterocorrelated 2D spectrum of **3** reveal the connectivities between the carbon and the proton signals (Table 6) in which each methylene carbon signal is seen to bear two diastereotopic protons. The methylene carbon resonances at 60.01 and 38.70 ppm for the uncoordinated arm of the amido triamine ligand were assigned by comparison with peaks observed at 58.89 and 40.17 ppm for H_3TMS-tren in C_6D_6,[15a] the coupling relationships between NH_a and methylene protons H_b and $H_{b'}$, as well as between methylene protons H_b, $H_{b'}$ and H_c, $H_{c'}$, and correlations between ^1H and ^{13}C chemical shifts (Table 6). The signals for the coordinated secondary amino branch were similarly assigned, thus leaving the remaining signals for assignment to the amido arm. The coordinated NH proton resonance is deshielded by 0.47 ppm compared to the uncoordinated NH signal.

Conclusions. Both compounds **2** and **3** display novel structural features among lithium amide compounds. Compound **2** constitutes an example of the unusual trigonal monopyramidal coordination environment for a metal. Although the Li−N bonds in **2** are quite labile as shown by VT NMR spectral studies, this technique indicates that **3** is quite rigid in solution, which may be a manifestation of the strength with which the LiCl moiety binds the two nitrogen-ligated lithium portions of the molecule together.

Acknowledgment. The authors are grateful to the National Science Foundation for a grant in support of this work. We are also grateful to Prof. George Sheldrick for helpful discussions regarding the twin refinement of **3**.

Supplementary Material Available: ORTEP diagrams and tables of crystallographic parameters, positional and thermal parameters, and bond lengths and angles for **2** and **3** (52 pages). Ordering information is given on any current masthead page.

IC9413631